Environment-assisted Quantum-enhanced Sensing with Electronic Spins in Diamond

Alexandre Cooper, Won Kyu Calvin Sun, Jean-Christophe Jaskula, and Paola Cappellaro

Phys. Rev. Applied **12**, 044047 — Published 21 October 2019

DOI: 10.1103/PhysRevApplied.12.044047

Environment-assisted quantum-enhanced sensing with electronic spins in diamond

Alexandre Cooper,[1,2] Won Kyu Calvin Sun,[1] Jean-Christophe Jaskula,[1] and Paola Cappellaro[1,*]

[1] *Department of Nuclear Science and Engineering and Research Lab of Electronics, Massachusetts Institute of Technology, Cambridge, MA 02139, USA*

[2] *Department of Physics, Mathematics and Astronomy, California Institute of Technology, Pasadena, CA 91125, USA*

(Dated: October 6, 2019)

The performance of solid-state quantum sensors based on electronic spin defects is often limited by the presence of environmental spin impurities that cause decoherence. A promising approach to improve these quantum sensors is to convert environment spins into useful resources for sensing, in particular entangled states. However, the sensitivity enhancement that can be achieved from entangled states is limited by experimental constraints, such as control errors, decoherence, and time overheads. Here we experimentally demonstrate the efficient use of an unknown electronic spin defect in the proximity of a nitrogen-vacancy center in diamond to achieve both an entangled quantum sensor and a quantum memory for readout. We show that, whereas entanglement alone does not provide an enhancement in sensitivity, combining both entanglement and repetitive readout achieves an enhancement in performance over the use of a single-spin sensor, and more broadly we discuss regimes where sensitivity could be enhanced. Our results critically highlights the challenges in improving quantum sensors using entangled states of electronic spins, while providing an important benchmark in the quest for entanglement-assisted metrology.

I. INTRODUCTION

Precision measurement of weak magnetic fields at the atomic scale is enabling novel applications in the physical and life sciences [1–3]. Electronic spin defects in solids with spin-dependent optical transitions are controllable quantum systems particularly suitable for such applications. In quantum sensing, an important challenge is to increase the sensitivity of spin sensors by taking advantage of their intrinsic quantum nature [4, 5] to realize, e.g., spin-squeezed states [6–8] or entangled states [9] of n spins, which, in the absence of limits imposed by decoherence, can in principle provide a gain in sensitivity up to $\sqrt{n}$ over the use of n independent spins [10, 11]. This gain in sensitivity is also expected when the sensing time is limited not by decoherence, but rather by external factors, such as is often the case in a.c. magnetometry experiments where the frequency of the measured field sets the acquisition time.

Achieving such a quantum enhancement in sensitivity, especially under realistic physical conditions, requires accessing ensembles of interacting spins that can be efficiently initialized, manipulated, and read out, as well as robustly prepared in entangled states with long coherence times. Magnetic sensing experiments with entangled states of electronic spins in solids have been so far prevented by the difficulty of accessing strongly-coupled spin systems that can be selectively addressed and robustly protected against the detrimental influence of environmental defects on their coherence and charge state properties.

Here, we explore an environment-assisted approach to quantum-enhanced sensing based on exploiting electronic spins in the environment of a well-characterized spin sensor [12, 13], such as those associated with crystalline defects [14–18], surface spins [19, 20], and paramagnetic labels [21, 22]. Besides increasing the number of sensing spins, combining diverse spin species enables distributing sensing tasks, e.g., for implementing multimodal sensing schemes where the primary spin is used for state preparation and read out, while auxiliary spins are used for sensing and storage. This approach bears resemblance to mixed-species quantum logic with trapped atomic ions [23, 24], where an auxiliary ion is used to cool, prepare, and read out the state of another ion, which in turn serves the role of a memory or a spectroscopic probe.

In particular, we investigate two strategies that could yield a quantum enhancement in sensing with the same qubit resource: (1) entanglement to improve its sensitivity to the parameter of interest, as well as (2) repetitive readout to increase the readout efficiency. We identify a regime of spin coupling strengths and entanglement decoherence rates for which entanglement provides an enhancement during sensing, even in the presence of control errors. We further take advantage of the fact that the proximal spin is robust against optical illumination to perform repetitive quantum measurements of its spin state to increase the readout efficiency. This last step is important to obtain a gain in performance, due to the large time overheads that generating and reading out entangled states introduce. Our results critically highlight the challenges of exploiting entanglement as a mean to achieve an enhancement in quantum sensing when accounting for the unavoidable increase in decoherence, control imperfections, and time overheads.

* pcappell@mit.edu

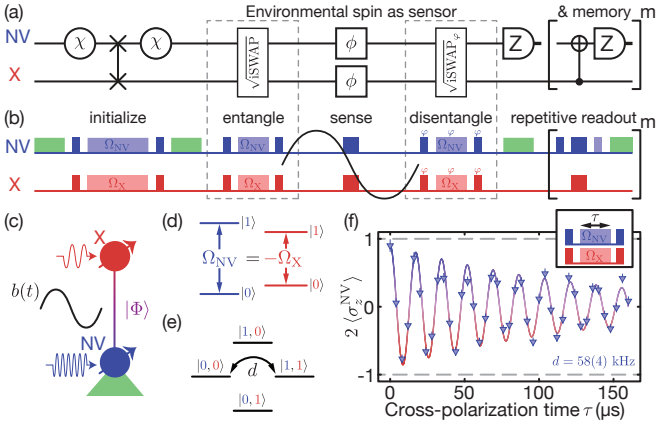

FIG. 1. **Environment-assisted quantum-enhanced sensing.** (a-c) Circuit, pulse sequence, and experimental system for sensing magnetic fields with a mixed entangled state of two electronic spins associated with a nitrogen-vacancy (NV) center and an electron-nuclear spin defect (X) in diamond. The two spins are polarized with a dissipative channel χ acting on the NV spin (green laser pulse) and a coherent spin-exchange gate between the NV and X spins (cross-polarization sequence). A mixed entangled state ρ_Φ, prepared with an entangling gate (cross-polarization sequence), acquires a coherent phase $\phi_\Phi = \phi_{NV} + \phi_X = 2\phi$, upon interacting with a sinusoidal magnetic field $b(t)$, which is then mapped as a population difference onto both the NV and X spins (cross-polarization sequence) and read out by performing a projective measurement on the NV spin (green laser pulse) and a series of m repetitive measurements on the X spin (recoupled spin-echo sequence). Resonant microwave pulses selectively drive the NV and X spins, whereas green laser pulses excite the NV spin for polarization and readout, while leaving the X spin unaffected. The phase of the pulses of the disentangling gate can be incremented at a constant rate to modulate the readout signal. (d-f) The spectrally mismatched spins are continuously driven at the Hartmann-Hahn matching condition, $|\Omega_{NV}| = |\Omega_X|$, to induce coherent spin exchange at the dipolar coupling strength $d = 58(4)$ kHz with a decay time of $T_{1\rho} = 132(11)$ μs.

II. QUANTUM CONTROL

We first develop coherent control techniques required to convert environmental spin defects into resources for sensing. While our control techniques are broadly applicable, here we demonstrate them on a system comprising two electronic spins, a single nitrogen-vacancy (NV) center and a proximal electron-nuclear spin defect (X) in diamond (Fig. 1a-c). The goal is to demonstrate the essential tools for environment-enhanced metrology, that is, initialization, control, and read out of the environmental (X) spin via the NV spin, as well as generation and characterization of quantum correlations, which are known to contribute to quantum enhancement in metrology.

The X defect is an environmental spin defect, with electronic spin-1/2 and nuclear spin-1/2, whose hyperfine and dipolar interaction tensors have been recently characterized [18]. A beneficial feature of this defect is that its spin state is not significantly perturbed by the NV optical readout (with a $T_1 > 270$ μs under laser illumination), enabling its use as a memory to perform repetitive quantum measurements. All experiments are performed at room temperature with a static magnetic field of 205.2(1) G aligned along the molecular axis of the NV center. Both NV and X spins are coherently controlled using resonant microwave pulses with a Rabi frequency of 1 MHz delivered through a coplanar waveguide. We drive the NV $|0\rangle$ and $|-1\rangle$ levels that we map to a qubit with states $|0\rangle$ and $|1\rangle$, respectively. We address only one of the two hyperfine transitions of the X spin to reduce control errors introduced when simultaneously driving both hyperfine transitions; further technical improvements in our radio-frequency pulse delivery system should enable mitigating such unwanted crosstalk. Because the X nuclear spin is unpolarized, addressing only one hyperfine transition halves the signal contrast. We renormalize the signal to this maximum contrast (by subtracting its baseline and multiplying by two), but analyze the performance of our approach for both an unpolarized and a fully polarized X nuclear spin.

A. State initialization via polarization transfer

Because the X spin, as many other environment spins, lacks a physical mechanism for state preparation, we initialize it by transferring polarization from the NV spin using a Hartmann-Hahn Cross-Polarization (HHCP) sequence [25, 26], during which both NV and X spins are continuously driven at the same Rabi frequency, $\Omega_{NV} = -\Omega_X$ (Fig. 1d). In the rotating frame the states $|0,0\rangle$ and $|1,1\rangle$ have the same energy (Fig. 1e), enabling coherent spin exchange at the dipolar coupling strength $d = 58(4)$ kHz between the NV and X spins, as observed in Fig. 1f after initializing the NV and X spins in the $|0,0\rangle$ state. We use the same cross-polarization sequence with an appropriate choice of driving phases to implement both polarization transfer gates (SWAP, $|00\rangle \mapsto |11\rangle$) and entangling gates ($\sqrt{\text{iSWAP}}$, $|00\rangle \mapsto (|00\rangle \pm i|11\rangle)/\sqrt{2}$) to prepare and detect two-spin coherence for sensing [27].

Using the HHCP sequence for a spin-exchange time of $\tau_{HHCP} = 8.6$ μs after a green laser initialization pulse, we perform N rounds of polarization transfer (Fig. 2a). The contrast of the cross-polarization signal increases from 49(3)% (N = 0) to 82(3)% (N = 1) and 88(4)% (N = 3), corresponding to an increase in X spin polarization from 14(3)% to 76(3)% and 94(6)% respectively. Because of the tradeoff between increasing polarization and reducing time overheads, we perform all of our experiments after a single round of polarization transfer.

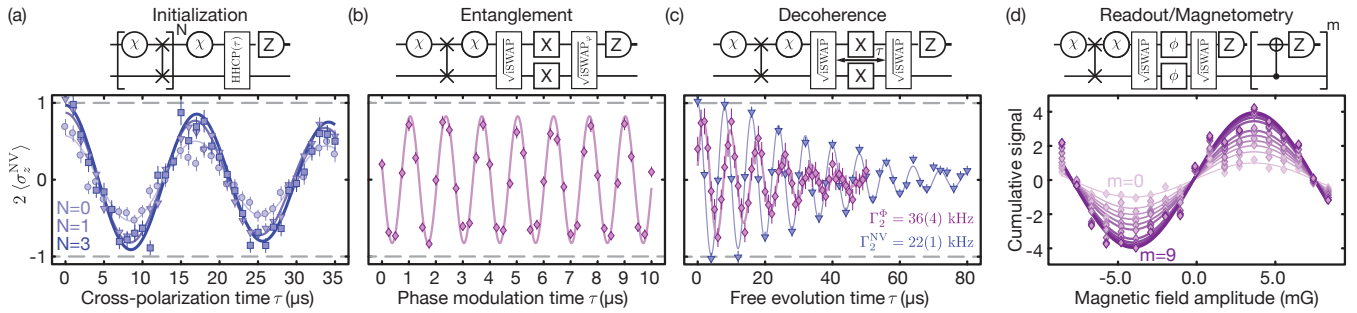

FIG. 2. **Quantum control.** (a) The increase in contrast of the cross-polarization signal after $N = 0$ (circle), $N = 1$ (triangle), and $N = 3$ (square) rounds of polarization transfer indicates an increase in X spin polarization from 14(3)% to 76(3)% and 94(6)% respectively. (b) The coherent oscillations of the signal measured after applying the entangling and disentangling gates indicate the preparation and detection of two-spin coherence with a contrast of 85(3)%. The phases of the pulses of the disentangling gate are modulated at 500 kHz and 250 kHz for the NV and X spins, such that the signal oscillates at 751(2) kHz, the sum of both frequencies. (c) The decay of the spin-echo signal (purple diamonds) for the mixed entangled state corresponds to a two-spin decoherence rate of $\Gamma_2^{\Phi} = 36(4)$ kHz, which is consistent with the sum of the decoherence rates for the NV spin (blue triangles, $\Gamma_2^{\mathrm{NV}} = 22(1)$ kHz) and X spin (not shown, $\Gamma_2^{\mathrm{X}} = 15(2)$ kHz). The coherent modulation is generated by incrementing the phase of the pulses of the disentangling gate rather than applying an external magnetic field. (d) Cumulative magnetometry signal measured for a sensing time of $\tau = 19$ μs using $m = 0$ (light purple diamonds) to $m = 9$ (dark purple diamonds) repetitive measurements of the X spin. The cumulative signal is normalized to the maximum amplitude of the magnetometry signal measured without repetitive measurements ($m = 0$). The cumulative signal contrast increases by a factor of 4.2 after $m = 9$ repetitive measurements, providing an increase in signal-to-noise ratio of 1.91(8) using optimal weights.

B. Entanglement generation and characterization

To generate entanglement between the spins, we then implement an entangling gate using the HHCP sequence for half the spin-exchange time of $\tau_{\mathrm{HHCP}}/2 = 4.3$ μs (Fig. 2b). Due to control imperfections in this maximally entangling gate and imperfect state preparation, we can only generate a mixed entangled state ρ_{Φ} [28]. Even if this is not the pure Bell entangled state, $|\Phi_{\pm}\rangle = (|00\rangle \pm i|11\rangle)/\sqrt{2}$, ρ_{Φ} has non-zero two-spin coherence in the subspace spanned by the Bell states, $C_{\Phi} = \sigma_x\sigma_y + \sigma_y\sigma_x$, more specifically, $\mathrm{tr}\,(\rho_{\Phi}C_{\Phi}) = 0.85(3)$ in each X-nuclear spin manifold, as determined by a parity measurement (see Appendix A). Though such mixed states are unavoidable due to control errors, they still prove to be useful to increase the precession rate of the two-spin sensor.

We characterize the two-spin coherence by converting it back into a population difference of the NV spin using a modulated disentangling gate; we modulate the phases of the pulses of the cross-polarization sequence acting on the NV and X spins at 500 kHz and 250 kHz to impart coherent oscillations at the sum of both frequencies [29, 30], simulating the evolution of two-spin coherence in the presence of a static magnetic field. As expected, the signal oscillates at 751(2) kHz, the sum of both frequencies, and the signal contrast is 85(3)%, consistent with the value measured after a single round of polarization transfer (Fig. 2b).

We further measure the coherence time of the single-spin and two-spin states (Fig. 2c) using a spin-echo sequence with decoupling pulses applied simultaneously to both NV and X spins. The coherence signal is fitted to $S(\tau) \propto e^{-(\Gamma_2\,\tau)^p}$, where Γ_2 is the decoherence rate and $p \approx 1.6$ is the decay exponent. We measure $\Gamma_2^{\mathrm{NV}} = 22(1)$ kHz, $\Gamma_2^{\mathrm{X}} = 15(2)$ kHz, and $\Gamma_2^{\Phi} = 36(4)$ kHz, such that the decoherence rate of the two-spin state is consistent with the sum of the decoherence rates of the NV and X spins, $\Gamma_2^{\Phi} = \Gamma_2^{\mathrm{NV}} + \Gamma_2^{\mathrm{X}}$. The NV and X spins experience different magnetic environments, such that $\Gamma_2^{\mathrm{X}} < \Gamma_2^{\mathrm{NV}}$, which is beneficial for achieving a gain in sensitivity using environmental spin defects.

C. Repetitive readout

We finally demonstrate repetitive readout of the X spin via the NV spin and show that the use of the X spin is beneficial for achieving an enhancement in the readout efficiency, given its resilience to optical illumination.

To measure the population state of the X spin, we can coherently map it onto the state of the NV spin, e.g., using a SWAP gate implemented using a cross-polarization sequence, as done for the experiments in Fig. 2a,c, or correlate it with the state of the NV spin, e.g., using a C-NOT gate implemented using a recoupled spin-echo sequence, as illustrated in Fig. 1b. Conversely, we can improve the NV spin readout by exploiting the X spin as a quantum memory, storing the desired information onto its state: as the X spin is stable under optical illumination, we can repeat multiple times the mapping and readout steps to increase the signal-to-noise ratio of the readout signal [31, 32].

Our approach has advantages over similar techniques exploiting nuclear spin ancillae [31, 32]: not only the optically-stable electronic spin is more robust than the ni-

trogen nuclear spin in the regime of low and intermediate static magnetic fields, but our strategy can be extended to optically addressable defects that, in contrast to the NV centers, do not possess an intrinsic nuclear spin. Fundamentally, we demonstrate that the same resources used for sensing can also enhance the central sensor readout.

In the current experiment with a single electronic spin ancilla, the amplitude of the optimally-weighted cumulative signal obtained for a magnetometry experiment at $\tau = 19$ μs increases by a factor of 4.2 after $m = 9$ additional repetitive measurements, providing an improvement in signal-to-noise ratio of 1.91(8) (Fig. 2d). We note that the number of repetitive measurements that provides an improvement in signal-to-noise ratio is not limited by the intrinsic relaxation of the X spin, but by imperfections in the gate used for the mapping. These results illustrate the advantage of working with environmental spins that are robust against optical illumination in such a way that they can be used as both quantum sensors for sensing magnetic fields and quantum memories whose state can be repetitively measured.

III. MAGNETIC FIELD SENSING

We now focus on the problem of estimating the amplitude of an external time-varying magnetic field whose temporal profile is known, here a sinusoidal field $b(t) = b\sin(2\pi\nu t)$. We sample the field with a phase-matched spin-echo sequence of duration $\tau = 1/\nu$ with decoupling pulses applied simultaneously on both spins. The average signal expected for n maximally entangled spins, which we assume are all equally coupled to the field, is given by $S_n(\tau) \propto \alpha_n(\tau)\sin(\nu_n(\tau)b)$, where $\nu_n(\tau) = n\gamma_e\hat{f}\tau$ is the precession rate of the interferometric signal, $\gamma_e = 2\pi$ 2.8 MHz is the gyromagnetic ratio of the electronic spin, and $\hat{f} \leq 2/\pi$ is a scaling factor quantifying the overlap between the sinusoidal field and the spin-echo sequence, with the equality held when the sinusoidal field and sampling sequence are phase-matched [1, 33–35].

We measure the magnetometry signal by sweeping the amplitude of the sinusoidal field (Fig. 3a) for sensing times $\tau = 2$, 10, and 19 μs. The signal shows coherent oscillations with the two-spin state precessing at twice the rate of the single-spin state. The relative difference in signal contrast is explained by decoherence during sensing and control errors (Fig. 3b). Indeed, the decrease in signal amplitude satisfies $\alpha_n(\tau) = \alpha_0^n e^{-(\Gamma_2^n\tau)^{p_n}}$, where Γ_2^n and p_n are the coherence parameters for n-spin states measured from independent spin-echo experiments (Fig. 2c). We estimate a nominal amplitude of $\alpha_0^{\mathrm{NV}} = 96(3)\%$ and $\alpha_0^{\Phi} = 78(6)\%$ for the single-spin and two-spin states, resulting from inefficiencies during state preparation and readout caused by dissipation and unitary control errors.

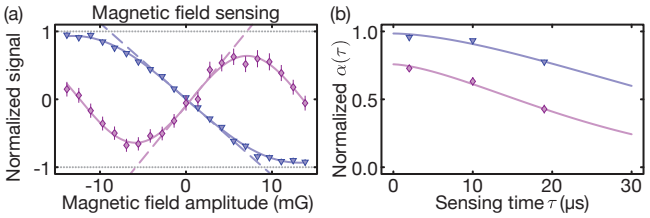

FIG. 3. **Magnetic sensing.** (a) Magnetometry signal measured with a single NV spin (blue triangles) and a mixed entangled state of two spins (purple diamonds) obtained by varying the amplitude of a sinusoidal magnetic field for a sensing time of $\tau = 10$ μs. The two-spin state precesses at twice the rate as the single-spin state. The sensitivity is proportional to the slope (dash lines) of the sinusoidal fit (solid curves). The magnetometry signal for the NV spin has been inverted for clarity. (b) The decrease in contrast of the magnetometry signal (normalized amplitude) for the single-spin state (blue triangles) and the two-spin state (purple diamonds) measured for a sensing time of $\tau = 2$, 10, and 19 μs is explained by decoherence during sensing (solid curves, which are fits to the echo decays in Fig. 2). The nominal loss in amplitude, $\alpha_0^{\mathrm{NV}} = 96(3)\%$ and $\alpha_0^{\Phi} = 78(6)\%$, is instead explained by dissipation and unitary control errors.

IV. PERFORMANCE ANALYSIS

We can now quantify the enhancement in performance achieved when sensing time-varying magnetic fields with an additional electronic spin, taking advantage of entanglement to increase the magnetic moment of the quantum sensor and repetitive read out to increase the readout efficiency.

To quantify the performance of the sensing protocol, the relevant figure of merit is the smallest amplitude of the magnetic field that can be measured by the n-spin sensor,

$$\delta b_n = \sigma_{S_n}/|dS_n(\tau)/db|, \tag{1}$$

where σ_{S_n} is the standard deviation of the magnetometry signal and $dS_n(\tau)/db = \alpha_n(\tau)\nu_n(\tau)$ is the maximum slope of the magnetometry signal (Fig. 3a). In practice, one is often interested in the smallest amplitude of the magnetic field that can be measured in a fixed time, which we define as the *sensitivity*

$$\eta = \delta b\sqrt{T}, \tag{2}$$

where $T = M(\tau + \tau_O)$ is the total experimental time for M measurements with a sensing time τ and time overheads τ_O.

To quantify the enhancement in δb_n that can be achieved when sensing with n spins instead of one we define the *gain in performance* as

$$g_n(\tau) = \delta b_1(\tau)/\delta b_n(\tau). \tag{3}$$

The gain in performance exceeds unity when the n-spin state outperforms the single-spin state and it is upper

bounded by the maximum gain in performance achieved in the absence of decoherence and control errors, i.e., $g \leq n$ if utilizing $(n-1)$ spin ancillas as sensors only. In our experiment, the gain in performance is given by $g_\Phi(\tau) = |\alpha_\Phi(\tau)\nu_\Phi(\tau)|/|\alpha_{\rm NV}(\tau)\nu_{\rm NV}(\tau)| \leq 2$. Here we safely assumed that the signal uncertainty σ_S is the same for the single-spin and two-spin sensing cases, as for both cases the signal is obtained by measuring the same NV and is limited by shot noise. The gain in performance is relevant in many scenarios, such as when the experiment can only be repeated for a fixed number of times due to external constraints on the duration or triggering of the magnetic waveform.

When instead time is an important resource, one can account for the increase in time overheads by defining the *gain in sensitivity* as

$$\tilde{g}_n(\tau) = g_n(\tau)h_n(\tau), \tag{4}$$

which quantifies the enhancement in the smallest amplitude of the magnetic field that can be achieved when sensing with n spins instead of one in a fixed time. Here $g_n(\tau)$ is the gain in performance defined above, and $h_n(\tau)$ is the relative time overheads needed to implement an n-spin protocol with more complex control requirements. We note that while $h_n(\tau)$ increases with τ (as the relative importance of time overheads decreases), $g(\tau)$ typically decreases with time, due to the faster decoherence of entangled states, $g(\tau) \propto e^{-(\Gamma_2^1\tau)^{p_1}}/e^{-(\Gamma_2^n\tau)^{p_n}}$. We thus generally expect to find an optimal sensing time where the gain in sensitivity is maximum and can exceed unity. In our experiment, $h_\Phi(\tau) = \sqrt{(\tau+\tau_{NV})/(\tau+\tau_{\rm NV}+\tau_\Phi)}$, where τ is the sensing time, $\tau_{\rm NV} = 5.7$ μs, and $\tau_\Phi = 21$ μs, which includes the additional time needed for state initialization, entanglement generation, and state readout, and scales inversely with the dipolar coupling strength.

A. Environmental spin as sensor

Our performance analysis results (Fig. 4a) show that, despite the twofold increase in precession rate, $|\nu_\Phi(\tau)/\nu_{\rm NV}(\tau)| = 2$ when using a mixed entangled state of two spins, the relative amplitude of the magnetometry signal is less than half, $|\alpha_\Phi(\tau)/\alpha_{\rm NV}(\tau)| \leq 1/2$ due to control errors, such that the use of entanglement does not provide a gain in performance and thus does not provide a gain in sensitivity. However, extrapolating our data to the case where we would use a fully polarized X nuclear spin or simultaneously drive both hyperfine transitions, we predict a gain in performance greater than unity for up to $\tau \approx 25$ μs. Still, when accounting for time overheads, there exists no sensing time for which a gain in sensitivity is achievable, unless our control imperfections were reduced by at least 8 %.

These results illustrate the fundamental tradeoff between increasing the number of spins and increasing control errors, decoherence rates, and time overheads. One approach to achieving a gain in sensitivity would be to improve the fidelity of our control operations or to look for a spin system with more favorable parameters. For instance, our simulation results illustrated in Fig. 4c show that, assuming the same level of control errors, a proximal spin defect with either stronger dipolar coupling $d \gtrsim 75$ kHz (reducing time overheads) or smaller decoherence rate, $\Gamma_2^{\rm X}/\Gamma_2^{\rm NV} \lesssim 0.4$ (increasing signal contrast at a given τ), is sufficient to achieve a gain in sensitivity using entanglement alone.

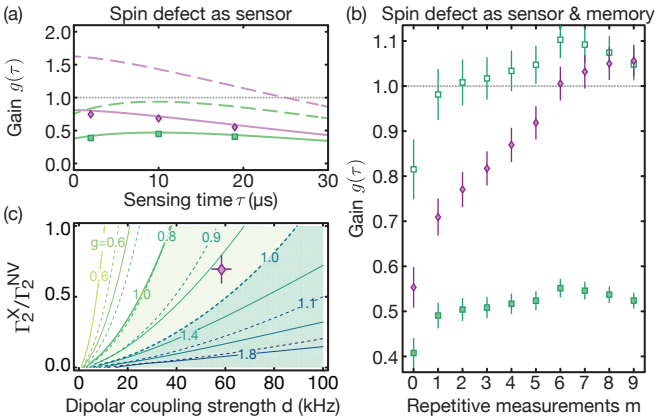

FIG. 4. **Performance analysis.** (a) Gain in performance (purple diamonds) and gain in sensitivity (green squares) measured for different sensing times before and after accounting for time overheads. Solid lines are extrapolated values estimated using our decoherence model. The expected gain in performance for a fully polarized X nuclear spin (dashed purple line) is greater than unity for up to ≈ 25 μs, but is less than unity for all times when accounting for time overheads (dashed green line). (b) Using the X spin as a memory for repetitive measurements improves the performance. The measured gain in performance (purple solid diamonds) before accounting for time overheads surpasses unity after $m = 6$ repetitive measurements and reaches a maximum of $g = 1.06(4)$ after $m = 9$ repetitive measurements. The measured gain in sensitivity maximizes to $\tilde{g} = 0.55(2)$ when accounting for time overheads (green solid squares); however, the extrapolated gain in sensitivity for a fully-polarized X nuclear spin achieves a maximum gain of $\tilde{g} = 1.10$ after $m = 6$ repetitive measurements. (c) Maximum gain in sensitivity achievable (dashed contour lines) for different values of the dipolar coupling strengths and relative decay rates of the two-spin system used for sensing. We assume a fully-polarized X nuclear spin, but use the control errors and NV coherence time measured experimentally. Without repetitive measurements, our two-spin system (purple diamond) lies outside the region where it outperforms a single spin (gain in performance $g > 1$, dark green region). With repetitive measurements (solid contour curves), the increase in signal-to-noise ratio, even after accounting for additional time overheads, shifts the boundary of the region of favorable performance, $g > 1$ (light green region), such that our two-spin system lies within it.

B. Environmental spin as memory

To further improve the enhancement in performance, we exploit the X spin as a memory that can store information about the measured field. The stored information can then be repetitively measured akin to quantum non-demolition measurement [36]. This approach results in an increased signal-to-noise ratio SNR(m) after m repetitive measurements and an upper bound for the gain in performance of $n\,\mathrm{SNR}(m)$. In our case, repetitive readout is enabled by the fact that, even at low static magnetic fields, the X spin is unperturbed by the optical pulse used to perform a projective measurement on the NV spin, providing an advantage over other ancillary spin systems such as nitrogen nuclear spins or nitrogen substitutional impurities (P1 centers). In addition, going beyond the typical repetitive readout scheme [31, 32], we take advantage of the fact that our disentangling gate maps the magnetic field-dependent phase as a population difference on both the NV and X spins. This provides a significant advantage, as it bypasses the need for an additional mapping operation, reducing both time overheads and the loss in signal contrast caused by control errors.

Using repetitive measurements of the X spins after sensing, we experimentally observe a two-fold maximum increase in SNR at both $\tau = 2$ and 19 μs, such that a gain in performance is achieved for the entire coherence time of the two-spin sensor. For sensing experiments at $\tau = 19$ μs (Fig. 4b), we achieve a gain in performance greater than unity after $m = 6$ repetitive measurements with a maximum of $g_{\mathrm{rr}} = 1.06(4)$ after $m = 9$ repetitive measurements. When accounting for the increased time overheads, using $\tau_\Phi \mapsto \tau_\Phi + (m-1)\tau_{\mathrm{rr}}$ with $\tau_{\mathrm{rr}} = 6.1$ μs, the gain in sensitivity maximizes to $\tilde{g}_{\mathrm{rr}} = 0.55(2)$ after $m = 7$ measurements when driving only one hyperfine transition of the unpolarized X nuclear spin. We however expect to reach $\tilde{g}_{\mathrm{rr}} = 1.10(4)$ for a fully polarized X nuclear spin or by driving both hyperfine transitions. Further gains in sensitivity could be achieved by accessing more strongly coupled spin systems with longer coherence times (see Fig. 4c), and reducing control errors, e.g., using optimal control techniques [37].

V. CONCLUSIONS

In conclusion, we have demonstrated an approach to quantum-enhanced sensing using entangled states of electronic spins by converting electron-nuclear spin defects in the environment of a single-spin sensor into useful resources for sensing, serving both as quantum sensors and quantum memories whose state can be repetitively measured. This approach complements ongoing efforts to improve the performance of single-spin sensors, including methods to limit the concentration of spin impurities [38, 39], extend coherence times with quantum error correction [40–43], increase the photon emission rate using Purcell effect methods [44–46], increase the collection efficiency using nanophotonic structures [47, 48], and increase the readout efficiency using spin-to-charge conversion techniques [49, 50]. We emphasize that while our experimental demonstration utilizes a previously unobserved spin system (X), our approach to quantum-enhanced sensing, and more generally to scaling up quantum registers, is applicable to any spin system, in particular environmental spin defects with favorable coupling strengths and coherence times. The techniques that we have developed are universally applicable to spin defects without a spin-dependent optical transition in diamond, including bulk defects such as P1 centers, spin defects on the surface of diamond, and paramagnetic labels in target molecules. These techniques can also be extended to other central spin defects that might not possess an intrinsic nuclear spin, such as silicon-vacancy centers in diamond or defects in silicon carbide. The dual use of a sensing spin as a memory bit would further require that it does not depolarize under a readout operation. For these general systems, we analyzed parameter regimes that can provide a gain in sensitivity.

We introduced coherent control techniques to initialize and repetitively read out an electronic spin defect, as well as to create an entangled state with two-spin coherence. We exploit these techniques to achieve a gain in performance in sensing time-varying magnetic fields and predict a gain in sensitivity for a fully polarized X nuclear spin, which is within experimental reach. The achieved gain in performance is significant for sensing applications where the magnetic waveform can only be triggered for a finite number of times or where the repetition time is much larger than the experiment time, such that time overheads are not limiting the acquisition rate. Still, we find that commonly encountered challenges associated with increased control errors, faster decoherence of entangled states, and additional time overheads limit the enhancement in performance achieved with entanglement alone. In particular, the additional time required for initialization, control and readout of the entangled state is especially deleterious, a practical fact often overlooked that our study helps highlighting. To at least partially overcome these challenges, we demonstrate that the environmental spin defect, which is resilient to optical illumination, can serve a dual role, not only acting as a magnetic field sensor, but also as a quantum memory, enabling repetitive readout of its spin state.

Finally, our results demonstrate that, despite the increased complexity and fragility, quantum control protocols can turn electronic spin defects in the environment of a single-spin sensor, usually considered as noise sources, into useful resources for realizing quantum-enhanced sensing. Further improvements in quantum control, such as optimal control techniques to improve gate fidelities [37], and materials properties, e.g., to deterministically create confined ensembles of interacting spin defects with slower decoherence rates and stronger coupling strengths, should enable achieving magnetic sensing beyond the standard quantum limit using elec-

tronic spin sensors.

VI. ACKNOWLEDGEMENTS

This work was in part supported by NSF grants PHY1415345 and EECS1702716. A. C. acknowledges financial support by the Fulbright Program and the Natural Sciences and Engineering Research Council of Canada. We are grateful to Chinmay Belthangady and Huiliang Zhang for their experimental support.

Appendix A: Phase modulation of the mixed entangled state

In order to characterize the mixed entangled state ρ_Φ and the two-spin quantum coherence created we modulate the state with σ_z rotations prior to mapping it onto a population of the NV spin. The mapping is achieved by performing the entangling gate $U_e = \sqrt{iSWAP}$, implemented by a HHCP sequence as explained in the main text, as this gate is effective in disentangling the two spins. More precisely, the disentangling gate allows a mapping from the two-spin coherences present in the mixed entangled state, $C_\Phi = \sigma_x\sigma_y + \sigma_y\sigma_x$, to the measurable observable, $\sigma_z^{\rm NV}$: $U_e\sigma_z^{\rm NV}U_e^\dagger = \frac{1}{2}(C_\Phi + \sigma_z^{\rm NV} - \sigma_z^X)$. Note that the two-spin coherences can be thought to arise from a combination of the two Bell-states $|\Phi_\pm\rangle$, $C_\Phi = |\Phi_+\rangle\langle\Phi_+| - |\Phi_-\rangle\langle\Phi_-|$. To extract the amplitude of C_Φ only, we exploit the fact that only this terms oscillates at twice the rate under a rotation around $(\sigma_z^{\rm NV} + \sigma_z^X)$. To implement such Z-rotation we borrow a technique from magnetic resonance (also exploited in the original Ramsey experiment), where the control gate phases are modulated. Since any driving around an axis at an angle ϕ in the x-y plane can be written as $e^{i\theta(\sigma_x\cos\phi+\sigma_y\sin\phi)} = e^{i\phi\sigma_z}e^{i\theta\sigma_x}e^{-i\phi\sigma_z}$, rotating all the phases of the driving fields implementing the disentangling gate U_e corresponds to applying an additional Z-rotation prior to it (we note that the final Z-rotation prior to detection has no effect on the chosen observable and can be dropped).

In the experiments shown in Fig. 2b, we applied a phase shift to the disentangling gate proportional to the time elapsed during the spin echo and with effective rates of 500 kHz and 250 kHz for the NV and X spins, such that the signal oscillates at 751(2) kHz, the sum of both frequencies. From the (normalized) amplitude of the oscillating part of the signal we can extract the amplitude of the C_Φ coherences to be 85(3)% in each nuclear spin manifold (that is, 0.43(2), when taking into account that the X nuclear spin is unpolarized).

[1] J. M. Taylor, P. Cappellaro, L. Childress, L. Jiang, D. Budker, P. R. Hemmer, A. Yacoby, R. Walsworth, and M. D. Lukin, "High-sensitivity diamond magnetometer with nanoscale resolution," Nature Physics **4**, 810–816 (2008).

[2] Romana Schirhagl, Kevin Chang, Michael Loretz, and Christian L. Degen, "Nitrogen-Vacancy Centers in Diamond: Nanoscale Sensors for Physics and Biology," Annual Review of Physical Chemistry **65**, 83–105 (2014).

[3] C. L. Degen, F. Reinhard, and P. Cappellaro, "Quantum sensing," Reviews of Modern Physics **89**, 035002 (2017).

[4] Todd Tilma, Shinichiro Hamaji, W. J. Munro, and Kae Nemoto, "Entanglement is not a critical resource for quantum metrology," Physical Review A **81**, 022108 (2010).

[5] Vittorio Giovannetti, Seth Lloyd, and Lorenzo Maccone, "Advances in quantum metrology," Nature Photonics **5**, 222–229 (2011).

[6] D. J. Wineland, J. J. Bollinger, W. M. Itano, F. L. Moore, and D. J. Heinzen, "Spin squeezing and reduced quantum noise in spectroscopy," Physical Review A **46**, R6797–R6800 (1992).

[7] James D. Macomber and Robert Lynch, "Squeezed spin states," The Journal of Chemical Physics **83**, 6514–6519 (1985).

[8] J. Estève, C. Gross, A. Weller, S. Giovanazzi, and M. K. Oberthaler, "Squeezing and entanglement in a BoseEinstein condensate," Nature **455**, 1216–1219 (2008).

[9] Jonathan A Jones, Steven D Karlen, Joseph Fitzsimons, Arzhang Ardavan, Simon C Benjamin, G Andrew D Briggs, and John J L Morton, "Magnetic Field Sensing Beyond the Standard Quantum Limit Using 10-Spin NOON States," Science **324**, 1166–1168 (2009).

[10] J. J . Bollinger, Wayne M. Itano, D. J. Wineland, and D. J. Heinzen, "Optimal frequency measurements with maximally correlated states," Physical Review A **54**, R4649–R4652 (1996).

[11] S. F. Huelga, C. Macchiavello, T. Pellizzari, A. K. Ekert, M. B. Plenio, and J. I. Cirac, "Improvement of Frequency Standards with Quantum Entanglement," Physical Review Letters **79**, 3865–3868 (1997).

[12] Marcus Schaffry, Erik M. Gauger, John J. L. Morton, and Simon C. Benjamin, "Proposed Spin Amplification for Magnetic Sensors Employing Crystal Defects," Physical Review Letters **107**, 207210 (2011).

[13] G. Goldstein, P. Cappellaro, J. R. Maze, J. S. Hodges, L. Jiang, A. S. Sørensen, and M. D. Lukin, "Environment-Assisted Precision Measurement," Physical Review Letters **106**, 140502 (2011).

[14] Fazhan Shi, Qi Zhang, Boris Naydenov, Fedor Jelezko, Jiangfeng Du, Friedemann Reinhard, and Jörg Wrachtrup, "Quantum logic readout and cooling of a single dark electron spin," Physical Review B **87**, 195414 (2013).

[15] M. S. Grinolds, M. Warner, K. De Greve, Y. Dovzhenko, L. Thiel, R. L. Walsworth, S. Hong, P. Maletinsky, and A. Yacoby, "Subnanometre resolution in three-dimensional magnetic resonance imaging of individual dark spins," Nature Nanotechnology **9**, 279–284 (2014).

[16] Helena S. Knowles, Dhiren M. Kara, and Mete Atatüre,

"Demonstration of a Coherent Electronic Spin Cluster in Diamond," Physical Review Letters **117**, 100802 (2016).

[17] E. L. Rosenfeld, L. M. Pham, M. D. Lukin, and R. L. Walsworth, "Sensing Coherent Dynamics of Electronic Spin Clusters in Solids," Physical Review Letters **120**, 243604 (2018).

[18] Alexandre Cooper, Won Kyu Calvin Sun, Jean-Christophe Jaskula, and Paola Cappellaro, "Spectral identification of electron-nuclear spin defects in diamond," (2018), arXiv:1807.00828.

[19] A. O. Sushkov, I. Lovchinsky, N. Chisholm, R. L. Walsworth, H. Park, and M. D. Lukin, "Magnetic resonance detection of individual proton spins using quantum reporters," Physical Review Letters **113**, 197601 (2014), arXiv:1410.3750.

[20] Sorawis Sangtawesin, Bo L Dwyer, Srikanth Srinivasan, James J Allred, Lila V H Rodgers, Kristiaan De Greve, Alastair Stacey, Nikolai Dontschuk, Kane M. O'Donnell, Di Hu, D Andrew Evans, Cherno Jaye, Daniel A Fischer, Matthew L Markham, Daniel J Twitchen, Hongkun Park, Mikhail D Lukin, and Nathalie P. de Leon, "Origins of diamond surface noise probed by correlating single spin measurements with surface spectroscopy," (2018), arXiv:1811.00144.

[21] Fazhan Shi, Qi Zhang, P. Wang, Hongbin Sun, J. Wang, Xing Rong, M. Chen, Chenyong Ju, Friedemann Reinhard, Hongwei Chen, Jörg Wrachtrup, J. Wang, and Jiangfeng Du, "Single-protein spin resonance spectroscopy under ambient conditions," Science **347**, 1135–1138 (2015).

[22] Lukas Schlipf, Thomas Oeckinghaus, Kebiao Xu, Durga Bhaktavatsala Rao Dasari, Andrea Zappe, Felipe Fávaro de Oliveira, Bastian Kern, Mykhailo Azarkh, Malte Drescher, Markus Ternes, Klaus Kern, Jörg Wrachtrup, and Amit Finkler, "A molecular quantum spin network controlled by a single qubit," Science Advances **3**, e1701116 (2017).

[23] P O Schmidt, "Spectroscopy Using Quantum Logic," Science **309**, 749–752 (2005).

[24] C. J. Ballance, V. M. Schäfer, J. P. Home, D. J. Szwer, S. C. Webster, D. T. C. Allcock, N. M. Linke, T. P. Harty, D. P. L. Aude Craik, D. N. Stacey, A. M. Steane, and D. M. Lucas, "Hybrid quantum logic and a test of Bell's inequality using two different atomic isotopes," Nature **528**, 384–386 (2015).

[25] S. R. Hartmann and E. L. Hahn, "Nuclear Double Resonance in the Rotating Frame," Physical Review **128**, 2042–2053 (1962).

[26] Abdelghani Laraoui and Carlos A. Meriles, "Approach to Dark Spin Cooling in a Diamond Nanocrystal," ACS Nano **7**, 3403–3410 (2013).

[27] Norbert Schuch and Jens Siewert, "Natural two-qubit gate for quantum computation using the XY interaction," Physical Review A **67**, 032301 (2003).

[28] V. Vedral, M. B. Plenio, M. A. Rippin, and P. L. Knight, "Quantifying Entanglement," Physical Review Letters **78**, 2275–2279 (1997).

[29] M. Mehring, J. Mende, and W. Scherer, "Entanglement between an Electron and a Nuclear Spin 1/2," Physical Review Letters **90**, 153001 (2003).

[30] Werner Scherer and Michael Mehring, "Entangled electron and nuclear spin states in N15@C60: Density matrix tomography," The Journal of Chemical Physics **128**, 052305 (2008).

[31] L. Jiang, J. S. Hodges, J. R. Maze, P. Maurer, J. M. Taylor, D. G. Cory, P. R. Hemmer, R. L. Walsworth, A. Yacoby, A. S. Zibrov, and M. D. Lukin, "Repetitive readout of a single electronic spin via quantum logic with nuclear spin ancillae," Science **326**, 267–272 (2009).

[32] Philipp Neumann, Johannes Beck, Matthias Steiner, Florian Rempp, Helmut Fedder, Philip R Hemmer, Jörg Wrachtrup, and Fedor Jelezko, "Single-Shot Readout of a Single Nuclear Spin," Science **329**, 542–544 (2010).

[33] G. de Lange, D. Ristè, V. V. Dobrovitski, and R. Hanson, "Single-Spin Magnetometry with Multipulse Sensing Sequences," Physical Review Letters **106**, 080802 (2011).

[34] Easwar Magesan, Alexandre Cooper, Honam Yum, and Paola Cappellaro, "Reconstructing the profile of time-varying magnetic fields with quantum sensors," Physical Review A **88**, 032107 (2013).

[35] A. Cooper, E. Magesan, H. N. Yum, and P. Cappellaro, "Time-resolved magnetic sensing with electronic spins in diamond," Nature Communications **5**, 3141 (2014).

[36] V B Braginsky, Y I Vorontsov, and K S Thorne, "Quantum Nondemolition Measurements," Science **209**, 547–557 (1980).

[37] Florian Dolde, Ville Bergholm, Ya Wang, Ingmar Jakobi, Boris Naydenov, Sébastien Pezzagna, Jan Meijer, Fedor Jelezko, Philipp Neumann, Thomas Schulte-Herbrüggen, Jacob Biamonte, and Jörg Wrachtrup, "High-fidelity spin entanglement using optimal control," Nature Communications **5**, 3371 (2014).

[38] Gopalakrishnan Balasubramanian, Philipp Neumann, Daniel Twitchen, Matthew Markham, Roman Kolesov, Norikazu Mizuochi, Junichi Isoya, Jocelyn Achard, Johannes Beck, Julia Tissler, Vincent Jacques, Philip R. Hemmer, Fedor Jelezko, and Jörg Wrachtrup, "Ultralong spin coherence time in isotopically engineered diamond," Nature Materials **8**, 383–387 (2009).

[39] G. Kucsko, S. Choi, J. Choi, P. C. Maurer, H. Zhou, R. Landig, H. Sumiya, S. Onoda, J. Isoya, F. Jelezko, E. Demler, N. Y. Yao, and M. D. Lukin, "Critical thermalization of a disordered dipolar spin system in diamond," Phys. Rev. Lett. **121**, 023601 (2018).

[40] G de Lange, Z H Wang, D. Riste, V V Dobrovitski, and R Hanson, "Universal Dynamical Decoupling of a Single Solid-State Spin from a Spin Bath," Science **330**, 60–63 (2010).

[41] Helena S. Knowles, Dhiren M. Kara, and Mete Atatüre, "Observing bulk diamond spin coherence in high-purity nanodiamonds," Nature Materials **13**, 21–25 (2014).

[42] E. M. Kessler, I. Lovchinsky, A. O. Sushkov, and M. D. Lukin, "Quantum Error Correction for Metrology," Physical Review Letters **112**, 150802 (2014).

[43] N. Bar-Gill, L.M. Pham, A. Jarmola, D. Budker, and R.L. Walsworth, "Solid-state electronic spin coherence time approaching one second," Nature Communications **4**, 1743 (2013).

[44] Luozhou Li, Tim Schröder, Edward H. Chen, Michael Walsh, Igal Bayn, Jordan Goldstein, Ophir Gaathon, Matthew E. Trusheim, Ming Lu, Jacob Mower, Mircea Cotlet, Matthew L. Markham, Daniel J. Twitchen, and Dirk Englund, "Coherent spin control of a nanocavity-enhanced qubit in diamond," Nature Communications **6**, 6173 (2015).

[45] Janine Riedrich-Möller, Sébastien Pezzagna, Jan Meijer, Christoph Pauly, Frank Mücklich, Matthew Markham, Andrew M. Edmonds, and Christoph Becher, "Nanoim-

plantation and Purcell enhancement of single nitrogen-vacancy centers in photonic crystal cavities in diamond," Applied Physics Letters **106**, 221103 (2015).

[46] Daniel Riedel, Immo Söllner, Brendan J. Shields, Sebastian Starosielec, Patrick Appel, Elke Neu, Patrick Maletinsky, and Richard J. Warburton, "Deterministic Enhancement of Coherent Photon Generation from a Nitrogen-Vacancy Center in Ultrapure Diamond," Physical Review X **7**, 031040 (2017).

[47] Thomas M. Babinec, Birgit J. M. Hausmann, Mughees Khan, Yinan Zhang, Jeronimo R. Maze, Philip R. Hemmer, and Marko Lončar, "A diamond nanowire single-photon source," Nature Nanotechnology **5**, 195–199 (2010).

[48] Noel H Wan, Brendan J Shields, Donggyu Kim, Sara Mouradian, Benjamin Lienhard, Michael Walsh, Hassaram Bakhru, Tim Schröder, and Dirk Englund, "Efficient Extraction of Light from a Nitrogen-Vacancy Center in a Diamond Parabolic Reflector," Nano Letters **18**, 2787–2793 (2018).

[49] B. J. Shields, Q. P. Unterreithmeier, N. P. de Leon, H. Park, and M. D. Lukin, "Efficient Readout of a Single Spin State in Diamond via Spin-to-Charge Conversion," Physical Review Letters **114**, 136402 (2015).

[50] Harishankar Jayakumar, Siddharth Dhomkar, Jacob Henshaw, and Carlos A. Meriles, "Spin readout via spin-to-charge conversion in bulk diamond nitrogen-vacancy ensembles," Applied Physics Letters **113**, 122404 (2018).